HAL
open science

Chirality of internal metallic and semiconducting carbon nanotubes

Revathi Bacsa, A. Peigney, Ch. Laurent, Pascal Puech, Wolfgang Bacsa

To cite this version:

Revathi Bacsa, A. Peigney, Ch. Laurent, Pascal Puech, Wolfgang Bacsa. Chirality of internal metallic and semiconducting carbon nanotubes. Physical Review B: Condensed Matter and Materials Physics (1998-2015), 2002, 65, pp.161404. 10.1103/PhysRevB.65.161404 . hal-00012442

HAL Id: hal-00012442

https://hal.science/hal-00012442v1

Submitted on 7 Jun 2023

HAL is a multi-disciplinary open access archive for the deposit and dissemination of scientific research documents, whether they are published or not. The documents may come from teaching and research institutions in France or abroad, or from public or private research centers.

L'archive ouverte pluridisciplinaire **HAL**, est destinée au dépôt et à la diffusion de documents scientifiques de niveau recherche, publiés ou non, émanant des établissements d'enseignement et de recherche français ou étrangers, des laboratoires publics ou privés.

arXiv:cond-mat/0111451v1 [cond-mat.mtrl-sci] 23 Nov 2001

Chirality of internal metallic and semiconducting carbon nanotubes

R.R. Bacsa[2], A. Peigney[2], Ch. Laurent[2], P. Puech[1], W.S. Bacsa [1*]

[1] *Laboratoire de Physique des Solides, UMR CNRS 5477, L'Institut de Recherche sur les Systmes Atomiques et Molculaires Complexes, Université Paul Sabatier, 118 route de Narbonne, 31062 Toulouse Cédex 4, France*

[2] *Centre Interuniversitaire de Recherche et d'Ingnierie des Matriaux, UMR CNRS 5085, Université Paul Sabatier, 118 route de Narbonne, 31062 Toulouse Cédex 4, France*

Abstract

We have assigned the chirality of the internal tubes of double walled carbon nanotubes grown by catalytic chemical vapor deposition using the high sensitivity of the radial breathing mode (RB) in inelastic light scattering experiments. The deduced chirality corresponds to several semiconducting and only two metallic internal tubes. The RB modes are systematically shifted to higher energies when compared to theoretical values. The difference between experimental and theoretical energies of the RB modes of metallic tubes and semiconducting tubes are discussed interms of the reduced interlayer distance between the internal and the external tube and electronic resonance effects. We find several pairs of RB modes corresponding to different diameters of internal and external tubes.

Typeset using REVTEX

Carbon nanotubes have unique properties due to their low dimensionality [1]. Numerous potential applications depend critically not only on the control of their chirality, diameter, number of layers and tube length but also on the development of high yield and low cost synthesis techniques [2]. It has been recently shown that the catalytic chemical vapor deposition (CCVD) technique based on transition metal oxides produces small diameter carbon nanotubes having $1-4$ walls with high yield and low cost [2]. The electronic and optical properties of the tubes are linked to their chirality and they can be semiconducting as well as metallic [1,6–9]. Metallic carbon nanotubes are considered to be model systems for one dimensional electronic transport where strong electronic correlations lead to collective low energy excitations [3,4]. Recent experimental reports suggest the existence of superconductivity in bundles of single walled carbon nanotubes [5]. Double walled carbon nanotubes (DWCNT) with an internal metallic tube and an insulating external tube could represent the ultimate one dimensional carbon based conductor. For DWCNT the chirality of the external tube can in principle be determined by scanning probe techniques or by electron or x-ray diffraction [10,11]. However, the determination of the chirality of the internal tube remains particularly challenging and has not been determined so far. The energy of the radial breathing (RB) mode in carbon nanotubes is inversely proportional to its diameter [18] which gives the possibility to find the diameter distribution using inelastic light scattering provided the scattering crosssection does not vary strongly with the tube diameter. For tube diameters smaller than $1nm$, the sensitivity of the radial breathing mode (RB) to the diameter is particularly high and ranges between $220-470cm^{-1}$/nm for a tube diameter between $1.0-0.7nm$ [18]. The chirality of the tubes can be explained by the fact that the honeycomb lattice can have different orientations with respect to the tube axis. For a given diameter range the number of different orientations possible for a honeycomb lattice is restricted to a finite number and can be found by the chiral vector specified by (n, m) [1]. The chiral vector connects equivalent points in the honeycomb lattice; its length determines the tube circumference and its direction gives the orientation with respect to the tube axis. For smaller diameters the number of unit cells forming the circumference decreases and

hence the number of tubes with different chirality within a given diameter range decreases. Combined with the higher sensitivity of the RB mode it becomes possible, provided the the observed RB modes are sufficiently narrow, to identify from the position of the RB mode the chirality of the tube .

Carbon nanotubes were prepared by the catalytic chemical vapor deposition method (CCVD) [2]. Selective reduction at 1000^oC in a methane-hydrogen ($18\%CH_4$) atmosphere of a solid solution of a transition metal oxide and an insulating oxide($Mg_{0.95}Co_{0.05}O$) led to the formation of small diameter carbon nanotubes with $1-4$ walls. After the reaction, the unreacted Co and MgO were dissolved in dilute (3.7%) hydrochloric acid and carbon nanotubes were recovered. High resolution electron microscopy images showed the presence of individual and bundles of nanotubes of diameters ranging from $0.6-3nm$. Most of them were single or double walled and were $> 100\mu m$ in length. Chemical analysis showed that the sample contained $95vol.\%$ of carbon.

We have selected a sample with mostly single and double walled tubes as verified by high resolution electron microscopy [12] with a significant fraction of internal tubes with diameters smaller than $1nm$ and we have examined the inelastic light spectrum of tubes along a single tube bundle. The tubes agglomerate to networks of bundles or ropes when deposited on a silica surface from a suspension [2,19]. We find that the packing of ropes depends on the diameter of the single and double walled tubes. The bundles have a variable diameter due to fact that they consist of tubes with different diameter and can on some locations consist of only a few tubes or one single tube. We have dispersed the tubes on a bilayer substrate to enhance the light scattering signal due to the enlarged local field [13]. This enhancement technique has the advantage in that it is not based on electronic resonance which can modify the spectra. We have used a micro-Raman spectrometer (DILOR XY, objective x100, spot size: $0.7\mu m$) with a micro-displacement stage to record successive spectra in steps of $0.5\mu m$ along a single tube bundle.

Raman scattering from vibrational modes of single wall carbon nanotubes have been reported earlier and have provided valuable structural and electronic information [20–22].

Strong in-plane covalent bonds and weak inter-planar interaction result in several in-plane modes in the range $1560-1600cm^{-1}$, a disorder induced band in the range $1300-1400cm^{-1}$ and out-of-plane (radial) modes at $< 400cm^{-1}$. The mode with the highest intensity at low energy is the radial breathing mode with symmetry A_{1g}. Modes of symmetry E_{2g} at low energy have not been observed so far due to their presumably low intensity [14]. Single wall CNT's grown by other techniques such as the pulsed laser evaporation [15] or the electric arc technique [16] have a typical diameter of $1.35nm$ and a RB mode at $157cm^{-1}$. We present here inelastic light spectra from DWCNT grown by the CCVD method with a significant fraction of tubes with small internal diameter tubes and RB modes between $150-370cm^{-1}$. While the electronic structure depends on tube diameter and chirality, the light scattering resonance is expected to follow the changes in the electronic structure of the tube. We have selected the 488nm line of the argon laser which is in resonance with metallic single walled tubes of diameter 0.95nm and semiconducting tubes of diameter $1.2nm$ [17]. All the tube-diameters have been determined by using the inverse relationship between diameter and RB energy [18].

Figure 1 shows spectra on two location on the sample in the energy range of the RB modes. The spectrum at the bottom shows a RB mode at $204cm^{-1}$ which corresponds to a diameter of 1.096nm and can be assigned to single walled tubes. Tubes with several different chiralities fall within the interval of the peakwidth and an assignment to one chirality cannot be made. The non-homogeneous line-shape is an indication that several diameters contribute to the observed peak. The spectrum at the top with two peaks at $167cm^{-1}$ and $302cm^{-1}$ is consistent with DWCNTs with external and internal diameters of 1.340nm and 0.741nm. The diameter of the internal tube is close to the diameter (0.747nm) which corresponds to the chirality (9,1) and (6,5). The two chiralities have by accident the same diameter and are both predicted to be semiconducting [1]. There are tubes with chirality (7,4) and (8,2) wih a similar diameter and they may also contribute to the observed band at $302cm^{-1}$. From the internal and the external diameter we find that the deduced interlayer distance (0.30nm) is smaller than in graphite (0.336nm).

We recorded several series of spectra along single bundles and we show here three spectra (figure 2) out of 50 along one tube bundle which have RB modes in the $280-350cm^{-1}$ range corresponding to tubes with particularly small diameter. We have indicated the calculated RB energies for all possible chiralities near the horizontal axis. The number of RB mode energies gets considerably smaller above $250cm^{-1}$. The spectrum at the bottom shows three main bands at $166cm^{-1}$, $202cm^{-1}$ and $300cm^{-1}$ with corresponding diameters of $1.35nm$, $1.1nm$ and $0.741nm$. The three peaks at $300cm^{-1}$ are narrower than in figure 1 and can be assigned to tubes of chirality (7,4), (9,1), (6,5) and (8,2). The tubes with chirality (7,4) and (8,2) both predicted to be metallic [1] fall within $1cm^{-1}$ of the predicted values (Table I). It is interesting to note that the peak at $302cm^{-1}$ which corresponds to two different chiralities both predicted to be semiconducting, has a larger intensity and is shifted to larger energies. We can pair the RB modes at $300cm^{-1}$ with RB mode at 166cm^{-1} and we deduce an interlayer spacing of $0.297-0.316nm$. In the spectrum in the middle of figure 2 we observe several RB modes between $150cm^{-1}$ and $343cm^{-1}$. We can assign the modes at $251cm^{-1}$ and $150cm^{-1}$ to double walled tubes corresponding to tube diameters of $0.89nm$ and $1.49nm$ and resulting interlayer spacing 0.3nm. The spectrum at the top of figure 2 shows several RB modes at higher Raman shifts ($336cm^{-1}$, $342cm^{-1}$ and $368cm^{-1}$). The RB modes in this range correspond to tubes of diameter $0.666nm$, $0.653nm$, $0.610nm$ which are particularly small and can be assigned to chiralities (8,1), (7,2) and (5,4). They can be associated to double walled tubes with RB modes of the external tube at $180cm^{-1}$ and the deduced interlayer spacing varies between $0.31-0.34nm$ for RB modes between $170-185cm^{-1}$.

While the peaks at $336cm^{-1}$ and $368cm^{-1}$ fall within $3cm^{-1}$ of the predicted values for tubes with chirality (8,1) and (5,4), the peak at $343cm^{-1}$ falls between the values for tubes with chirality (8,1) and (7,2) (Table I) and could be associated with either of the two. In fact an increased bond length due to the higher curvature would shift the RB modes to lower energy but this should also be observed for the other tubes in the same diameter range. A reduced interlayer spacing would lead to a compression of the internal tube in a DWCNT

and could explain the upshift of the RB mode.

Recently, doubled walled CNT's have been synthesized through high temperature annealing (1200^oC) of single walled tubes filled with C_{60} [29]. The Raman spectra using the $514.5nm$ excitation of these tubes showed additional bands at $260cm^{-1}$, $315cm^{-1}$ and $377cm^{-1}$ with line widths of $> 8cm^{-1}$. The diameter difference of inner and outer diameter (0.71nm) or interlayer distance (0.36nm) was found to be systematically larger than in graphite (0.335nm) in contrast to our findings here on catalytic CVD grown DWCNTs.

A systematic up-shift of the RB modes of single walled CNT's has been associated to intertubular interaction and distortion in bundles [23] and theoretical calculations indicate a up-shift of upto 10% for tubes in bundles [24]. Furthermore a theoretical study has recently shown that gas absorption within the interstitial channels of a bundele of CNTs can increase the RB mode energy [25,26] by 2.7%. This can certainly influence the position of the RB modes of the external tunbes but less likely the RB modes of the internal tubes. Taking into account the influence of the neighboring tubes on the RB mode of the external tube we find that the deduced interlayer spacing is larger ($0.32nm$) and brings the interlayer spacing closer to graphite.

Table I shows that the differences between the experimental and theoretical values of the RB modes are different for semiconducting and metallic tubes. This difference can be explained by resonace effects, sensitive to changes in the electronic structure of the tube. Inelastic light spectra of single shell carbon nanotubes [27] and of our DWCNT taken with an excitation source at $488.0nm$ have been found to be downshifted compared to spectra taken at $514.5nm$ and this can explain the differences observed for two types of DWCNT's. But the deduced different interlayer distance in the two types of double walled tubes could also indicate differences in the growth mechanism of catalytic CVD grown and annealed doubled walled tubes. Annealing causes a growth of an internal tube whereas in the CVD method presumably the external tube grows on the inner tube. This is consistent with the tendency that the layer grown later in the process forms before an interlayer distance corresponding to the value observed in graphite is reached.

Among the observed chiralities of the internal tubes we have found neither a zigzag (n,0) nor a armchair (n,n) tube and in the diameter range of the internal tubes we find among the chiralities which have not been observed, three semiconducting and three metallic tubes. This fact indicates that the growth of the tubes with chiralities other than zigzag or armchair may be favored due to their lower symmetry. Finally we note the particlularly narrow line shape of some of the RB modes of the internal tubes which in fact made it possible to assign the chirality of the tubes. The dispersion of the tubes on the bilayer substrate and selection of a single tube bundle using a microscope has the effect to reduce the broadening due to size dispersion. The narrow line shape shows the high coherence length and harmonicity for RB modes of internal tubes. The RB modes are localized on a very narrow tube and we expect that DWCNT's are as a result exceptionally good thermal conductors.

We have observed RB modes of DWCNTs by inelastic light scattering. The narrow diameter of the internal tubes grown by the catalytic CVD method, the higher sensitivity of the RB mode for smaller diameter and the reduced number of chiral vectors in this diameter range as well as the narrow line widths made it possible to assign the chirality of the internal tubes. We observe two metallic as well as several semiconducting tubes and no zigzag (n,0) or armchair (0,m) tubes. Differences between experimental and theoretical energies of the RB modes are found to be larger for semiconducting tubes and attributed to mostly electronic resonance effects.

Acknowledgement:

We would like to thank A. Zwick for helpful discussions and R. Sirvin for technical support.

REFERENCES

* e-mail: wolfgang.bacsa@lpst.ups-tlse.fr

[1] M.S. Dresselhaus, G. Dresselhaus, P.C. Eklund, The Science of Fullerenes and Carbon Nanotubes, Academic Press (1995)

[2] R.R. Bacsa, Ch. Laurent, A. Peigney, W.S. Bacsa, Th. Vaugien, A. Rousset, Chem. Phys. Lett. **323**, 566 (2000)

[3] R.Egger and A. Gogolin, Phys. Rev. Lett. **79**, 598 (1997), R. Egger, Phys. Rev. Lett. **83**, 5547 (1999)

[4] C. Kane, L. Balents, and M.P. Fisher, Phys. Rev. Lett. **79**, 5089 (1997)

[5] M. Kociam, A.Y. Kasumov, S. Gueron, B. Reulet, I.I. Khodos, Y.B. Gorbatov, V.T. Volkov, L. Vaccarini, and H. Bouchiat, Phys. Rev. Lett. **86**, 2416 (2001)

[6] N. Hamada, S.I. Sawada, A. Oshiyama, Phys. Rev. Lett. **68**, 1579 (1992)

[7] J.W.G. Wildoer et. al. , Nature (London) **391**, 59 (1998)

[8] M. Bockrath, D.H. Cobden, J. Lu, A.G. Rinzler, R.E. Smalley, L. Balents and P.L. McEuen, Nature, **397**, 598-602 (1999)

[9] S. Tasaki, K. Meakawa, T. Yamabe Phys. Rev. B **57**, 9301 (1998)

[10] Teri Wang Odom, Jin-Lin Huang, Philip Kim and Charles M. Lieber, Nature **391**, 62-64 (1998)

[11] R.R. He, H.Z. Jin, J. Zhu, Y.J. Yan, X.H. Chen, Chem. Phys. Lett. **298**, 170 (1998)

[12] Statistical analysis on 67 isolated nanotubes of the same sample showed that 38% of the tubes are single walled, 58% double walled and the remaining having three or four walls. In the smallest diameter range (0.8-1.0nm) we find only double walled tubes.

[13] W.S. Bacsa and J.S. Lannin, Appl. Phys. Lett. Vol. **61**, 19 (1992)

[14] R. Saito, T. Takeya, T. Kimura, G. Dresselhaus, M.S. Dresselhaus, Phys. Rev. B **57**, (1998) 4145

[15] A. Thess et al. Science **273**, 483 (1996)

[16] C. Journet et al. Nature **388**, 756 (1997)

[17] Y.F. Wang, X.W. Cao, S.F. Hu, Y.Y. Liu, G.X. Lan, Chem. Phys. Lett. **336**, 47 (2001)

[18] S. Bandow, S. Asaka, Y. Saito, A.M. Rao, L. Grigorian, E. Richter, P.C. Ecklund, Phys. Rev. Lett. **80**, 3779 (1998)

[19] M. Terrones, H. Terrones, F. Banhart, J. -C. Charlier and P. M. Ajayan, Science, **288**, 1227, 2000

[20] E. Richter and K.R. Subbaswamy, Phys. Rev. Lett. **79**, 2738 (1997)

[21] A.M. Rao et al., Science **275**, 187 (1997)

[22] W.S. Bacsa, W. Walter, S. Awadallah, S. Mcginnis, J.W. Ager, K. Parvin and R.S. Ruoff, Proceedings of the symposium on Recent Advances in Chemistry and Physics of Fullerenes and Related Materials **3**, 749, (1996)

[23] U.D. Venkateswaran, A.M. Rao, E. Richter, M. Menon, A. Rinzler, R.E. Smalley, P.C. Eklund, Phys. Rev. B **59**, 10928, (1999)

[24] L. Henrard, E. Hernandez, P. Bernier, A. Rubio, Phys. Rev. B **60**, R8521 (1999)

[25] M.M. Calbi, F. Toigo, M.W. Cole Phys. Rev. Lett. **86**, 5062 (2001)

[26] W. Teizer, R.B. Hallock, E. Dujardin, T.W. Ebbesen **82**, 5305 (1999)

[27] Ping Heng Tan et al. Appl. Phys. Lett. **75**, 1524 (1999)

[28] A.M. Rao, J. Chen, E. Richter, U. Schlecht, P.C. Eklund, R.C. Haddon, U.D. Venkateswaran, Y.K. Kwon, D. Tomanek, Phys. Rev. Lett. **86**, 3895, (2001)

[29] K. Hiranhana, K. Suenaga, S. Bandow, H. Kato, T. Okazaki, H. Shinohara, S. Iijima, Phys. Rev. Lett. **85**, 5384, (2000)

Table

TABLES

TABLE I. Experimental and predicted RB energies

experiment	theory	difference	diameter	chirality
cm^{-1}	cm^{-1}	cm^{-1}	nm	(n, m)
297.0	296.2	0.8	0.756	(7,4) metallic
302.0	299.4	2.6	0.747	(9,1),(6,5) semiconducting
312.0	311.6	0.4	0.718	(8,2) metallic
336.0	334.3	1.7	0.669	(8,1) semiconducting
342.0	348.9	-6.9	0.641	(7,2) semiconducting
368.0	365.7	2.3	0.612	(5,4) semiconducting

Figure Captions

1. Room temperature Raman spectra of RB modes on two location of the sample. The spectrum at the bottom is assigned to mostly single walled tubes and the spectrum at the top can be assigned to mostly double walled carbon nanotubes.

2. Room temperature Raman spectra of RB modes along a tube bundle containing double walled carbon nanotubes with different internal and external diameters.

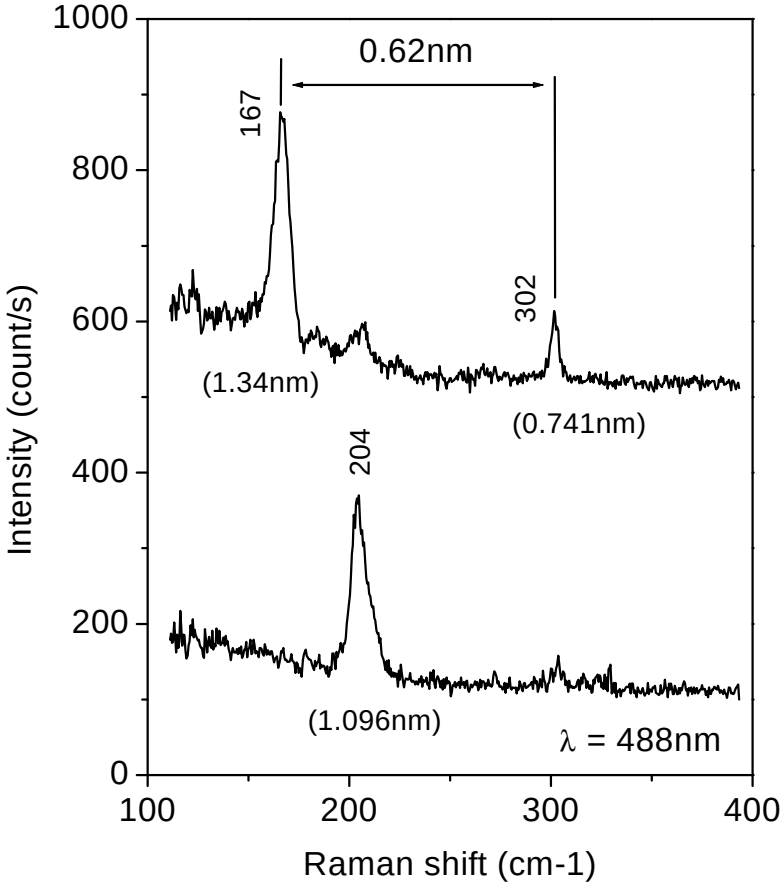
1000
800
600
400
200
0
Intensity (count/s)
100
200
300
400
Raman shift (cm-1)
0.62nm
167
302
(1.34nm)
(0.741nm)
204
(1.096nm)
λ = 488nm

Fig 1

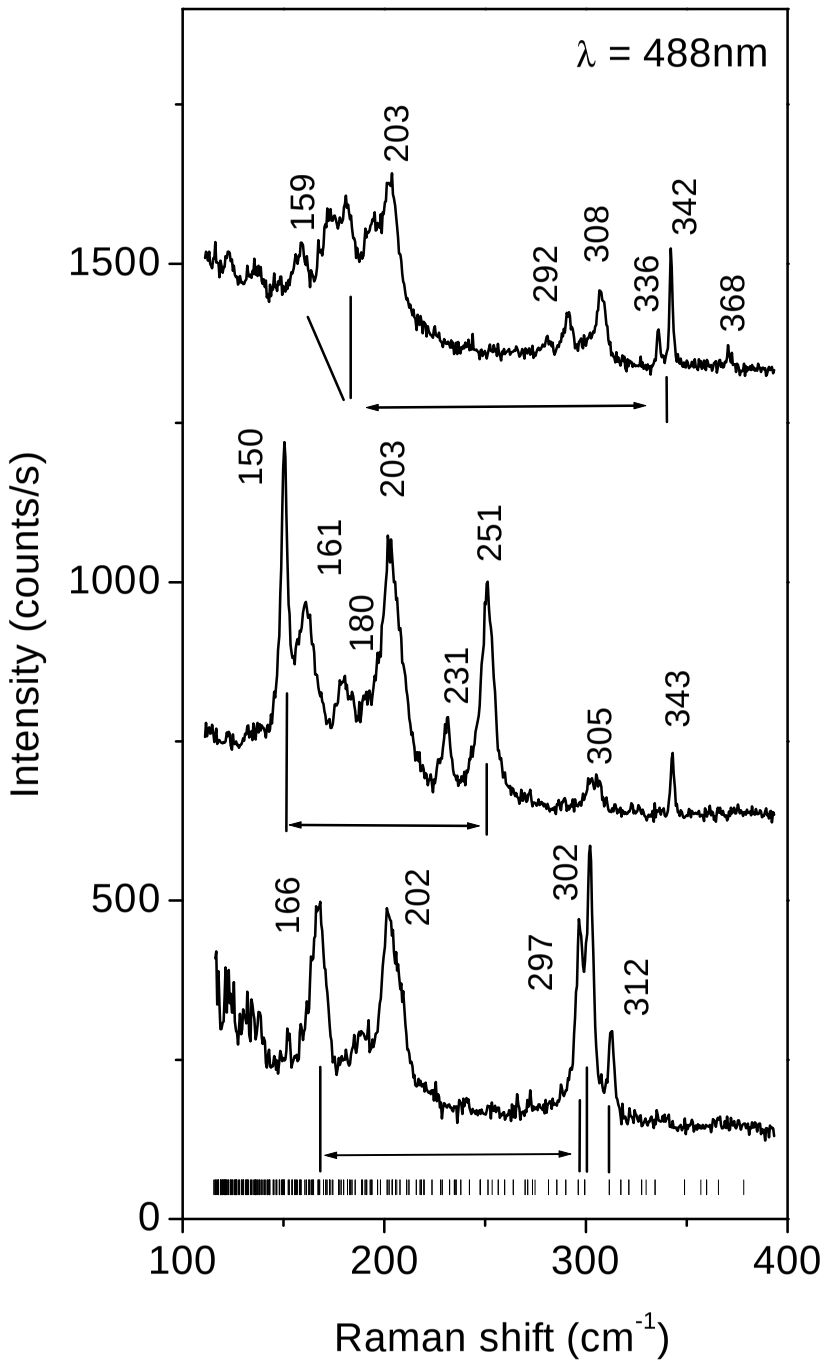
λ = 488nm
Intensity (counts/s)
Raman shift (cm-1)
0
500
1000
1500
100
200
300
400
159
203
292
308
336
342
368
150
161
180
203
231
251
305
343
166
202
297
302
312

Fig 2